

# Probing $f(R)$ gravity with PLANCK data on cluster pressure profiles

I. De Martino<sup>1,4</sup>, M. De Laurentis<sup>2,3,4</sup>, F. Atrio-Barandela<sup>1</sup>, S. Capozziello<sup>3,4</sup>

<sup>1</sup> Física Teórica, Universidad de Salamanca, 37008 Salamanca, Spain;

<sup>2</sup>Department of Theoretical Physics, Tomsk State Pedagogical University (TSPU), pr. Komsomolsky, 75, Tomsk, 634041, Russia;

<sup>3</sup> Dipartimento di Fisica, Università di Napoli "Federico II";

<sup>4</sup>INFN sez. di Napoli Compl. Univ. di Monte S. Angelo, Edificio G, Via Cinthia, I-80126 - Napoli, Italy.

E-mail: [ivan.demartino@usal.es](mailto:ivan.demartino@usal.es)

**Abstract.** Analytical  $f(R)$ -gravity models introduce Yukawa-like corrections to the Newtonian potential in the weak field limit. These models can explain the dynamics of galaxies and cluster of galaxies without requiring dark matter. To test the model, we have computed the pressure profile of 579 X-ray galaxy clusters assuming the gas is in hydrostatic equilibrium within the potential well of the modified gravitational potential. We have compared those profiles with the ones measured in the foreground cleaned SMICA released by the Planck Collaboration. Our results show that Extended Theories of Gravity explain the dynamics of self-gravitating systems at cluster scales and represent an alternative to dark matter haloes.

## 1. Introduction

The Cosmic Microwave Background (CMB) temperature anisotropies measured by the Wilkinson Microwave Anisotropy Probe (WMAP) [2] and the Planck satellites [3, 4, 5, 6] as well as luminosity distances measured of the Supernovae Type Ia (SNeIa) [1], strongly favor the concordance  $\Lambda$ CDM model, where the Universe is dominated by two unknown energy densities: Dark Energy (DE) and Dark Matter (DM). As an alternative, analytical  $f(R)$ -models modify the description of gravity instead of requiring extra matter components. In these extensions of General Relativity (GR), the Hilbert-Einstein action is replaced with a more general function of the Ricci scalar  $R$  [7]. These models have been found to introduce negligible corrections at the scale of the Solar systems [8] so they verify the constraints imposed by the classical test of GR, and the perturbations in self-gravitating systems behave similarly as in GR [9]. Nevertheless, this modified gravity introduces a Yukawa-like correction to the gravitational potential in the Post-Newtonian limit [7, 10]. This modified potential has been used to explain the dynamics of galaxies without requiring DM [11, 12].

Since, the exact functional form of the Lagrangian is unknown, it is important to test potential models using all the available data on self-gravitating systems. Galaxy clusters are reservoirs of hot gas and when CMB photons cross the cluster potential well, they are scattered off by the free electron of the intracluster medium. The effect, known as Sunyaev-Zeldovich (SZ) [13, 14], induces secondary anisotropies that have been extensively measured [15, 16, 5, 17].

Pressure profiles of cluster of galaxies based on the Navarro-Frenk-White (NFW, [18]) DM density profile have been found to be in agreement with SZ [19] and X-ray observations [20]. We have constructed the pressure profiles of clusters of galaxies assuming the gas is in hydrostatic equilibrium within a Newtonian potential with a Yukawa correction and compared them with Planck data. This article is organized as follows: in Sec. 2, we describe the weak field limit of  $f(R)$  gravity; in Sec. 3, we summarize the pressure profiles most commonly used in the literature and compare them with the pressure profile for  $f(R)$  models; in Sec. 4 we describe the data used in our analysis; in Sec. 5 we present our results and in Sec. 6 we will summarize our main conclusions.

## 2. Yukawa corrections to the Newtonian potential in $f(R)$ -gravity

In Extended Theories of Gravity (ETGs), the field equations are obtained by varying the action

$$\mathcal{A} = \frac{c^4}{16\pi G} \int d^4x \sqrt{-g} f(R) + \mathcal{L}_m, \quad (1)$$

resulting in <sup>1</sup>

$$f'(R)R_{\mu\nu} - \frac{f(R)}{2} g_{\mu\nu} - f'(R)_{;\mu\nu} + g_{\mu\nu} \square_g f(R) = 8\pi G T_{\mu\nu}.$$

To construct spherically symmetric solutions, we write the metric element as

$$ds^2 = g_{tt}c^2 dt^2 - g_{rr} dr^2 - r^2 d\Omega, \quad (2)$$

where  $d\Omega$  is the solid angle. We restrict our study to  $f(R)$ -Lagrangians that are expandable in Taylor series around a fixed point  $R_0$

$$f(R) = \sum_n \frac{f^{(n)}(R_0)}{n!} (R - R_0)^n \simeq f_0 + f'_0 R + \frac{f''_0}{2} R^2 + \dots \quad (3)$$

In the Post-Newtonian limit of these models the gravitational potential can be written as [7]

$$\Phi_{grav}(r) = \frac{\Phi_N(r)}{(1 + \delta)} \left( 1 + \delta e^{-\frac{r}{L}} \right). \quad (4)$$

In this expression,  $\delta$  represents the deviation from GR at zero order and the Newtonian limit of GR is recovered at  $\delta \rightarrow 0$ , irrespective of the scale parameter  $L$ . The latter is the scale length of the self-gravitating object [7, 10] and its effects are negligible at Solar System scales where GR, is restored [10]. In terms of the coefficients in the Taylor expansion they are given by  $\delta = 1 - f'_0 = 1$  and  $L = [-f'_0/(6f''_0)]^{1/2}$ . In this context, the dynamical effects of DM are now given by the modifications of the Newtonian potential.

## 3. Cluster pressure profiles in $f(R)$ gravity

SZ effect induces two different type of secondary temperature anisotropies on the CMB: a thermal contribution due to the motion of the electrons within the cluster potential well and a kinematic one (KSZ) due to the peculiar motion of the cluster. It is given by

$$\frac{\Delta T}{T_0} = g(\nu) \frac{k_B \sigma_T}{m_e c^2} \int n_e T_e dl, \quad (5)$$

<sup>1</sup>  $f'(R) = df(R)/dR$  is the first derivative with respect to the Ricci scalar,  $\square_g = ;_{\sigma}{}^{\sigma}$  is the d'Alembertian with covariant derivatives,  $T_{\mu\nu} = -2(-g)^{-1/2} \delta(\sqrt{-g} \mathcal{L}_m) / \delta g^{\mu\nu}$  is the matter energy-momentum tensor,  $T$  its trace,  $g$  the determinant of the metric tensor  $g_{\mu\nu}$ . Greek indices run from 0 to 3.

Table 1: Parameters of the GNFW corresponding to [20, 15, 24],  $\beta$  for Coma cluster and  $f(R)$  is the best fit model to Planck data.

<i>Model</i>	$c_{500}$	$\alpha_a$	$\beta_a$	$\gamma_a$	$P_0$
<i>Arnaud</i>	1.177	1.051	5.4905	0.3081	$8.403h_{70}^{3/2}$
<i>Planck</i>	1.81	1.33	4.13	0.31	6.41
<i>Sayers</i>	1.18	0.86	3.67	0.67	4.29

---

$\beta$	$\beta$	$n_{e,0}/m^{-3}$	$r_c/\text{Mpc}$	$T_e/\text{keV}$
	2/3	3860.	0.25	6.48

---

$f(R)$	$\delta$	L/Mpc	$\gamma$
	-0.98	0.1	1.2

where  $T_e$  is the electron temperature,  $n_e$  the electron density and the integration is carried out along the line of sight  $l$ . In Eq. (5)  $k_B$  is the Boltzmann constant,  $m_e c^2$  the electron annihilation temperature,  $c$  the speed of light,  $\nu$  the frequency of observation,  $\sigma_T$  the Thomson cross section and  $T_0$  the mean temperature of the CMB. Finally,  $g(\nu) = x \coth(x/2) - 4$  is the frequency dependence of the TSZ effect, with the reduced frequency  $x = h\nu/KT_0$ . For individual clusters, only the TSZ anisotropy has been measured.

Eq. (5) shows that in order to compute the TSZ anisotropies we need to estimate the cluster pressure profile,  $n_e T_e$ . Several cluster profiles, based on X-ray data and numerical simulations, have appeared in the literature:

- The isothermal  $\beta$ -model [21, 22] specifies the electron density:  $n_e(r) = n_{e,0}[1+(r/r_c)^2]^{-3\beta/2}$ . From X-ray surface brightness data it has been found that  $\beta = 0.6 - 0.8$  [23].
- The universal profile [20] is a phenomenological model based on the NFW DM-profile

$$p(x) \equiv \frac{P_0}{(c_{500}x)^{\gamma_a} [1 + (c_{500}x)^{\alpha_a}]^{(\beta_a - \gamma_a)/\alpha_a}}, \quad (6)$$

where  $x$  is the radial distance in units of  $r_{500}$ , the radius where the average density is 500 times the critical density, and  $c_{500}$  is the concentration parameter at  $r_{500}$ . Different groups have fit the model parameters  $[c_{500}, \alpha_a, \beta_a, \gamma_a, P_0]$  to X-ray or CMB data; their best fit values are given in Table 1.

To compute in  $f(R)$  gravity the pressure profile  $n_e T_e$  of Eq. (5) we assume that the gas is in hydrostatic equilibrium within the modified potential well of the cluster (without the DM contribution)

$$\frac{dP(r)}{dr} = -\rho(r) \frac{d\Phi_{grav}(r)}{dr}, \quad (7)$$

and the physical state of the gas is described by a polytropic equation of state

$$P(r) \propto \rho^\gamma(r). \quad (8)$$

Eqs. (7) and (8), together with the continuity equation

$$\frac{dM(r)}{dr} = 4\pi\rho(r), \quad (9)$$

and the cluster gravitational potential given by eq. (4) form a close system that can be solved numerically to obtain the pressure profiles of any given cluster as a function of two gravitational parameters ( $\delta, L$ ) and the polytropic index  $\gamma$ . Fig. 1 we represent the different profiles integrated along the line of sight with the parameters given in Table 1. The profiles are particularized for the parameters of the Coma cluster.

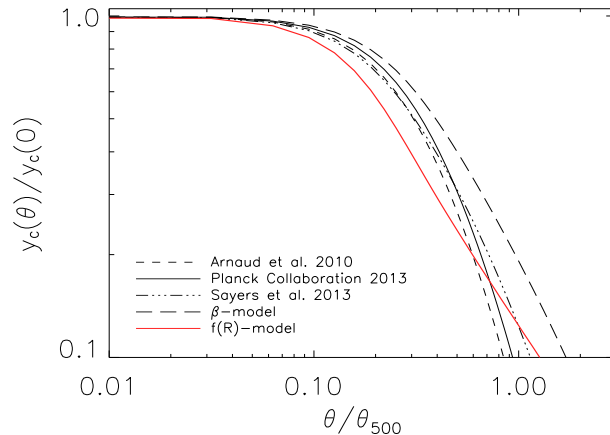


Figure 1: Pressure profiles integrated along the line of sight for the Coma cluster ( $z = 0.023$ ). We plot three GNFW profiles (dashed, solid and dash-dotted lines), one  $\beta = 2/3$  model (long dashed line) and a  $f(R)$  model (red solid line). The parameters of each model are given in Table 1.

#### 4. Data.

We use Planck data and a X-ray selected cluster catalog to constrain the pressure profiles of clusters of galaxies.

- Our cluster catalog is fully described in [25] and lists position, redshift, X-ray flux, X-ray luminosity. The X-ray electron temperature is derived from the  $L_X - T_X$  relation of [26]. A total of 579 clusters are located outside the minimal Planck mask; the region where the CMB data is less affected by galactic foreground residuals.

- The Planck Collaboration released in March 2013 nine maps of the CMB temperature anisotropies spanning a frequency range from 30 to 845 GHz. Since foreground cleaned maps at all frequencies were not made available, we performed our analysis on a foreground cleaned map known as SMICA. This map has been constructed using a component separation method by combining the data at all frequencies [27]. The SMICA map has  $5'$  resolution.

For all except the brightest clusters, the underlying CMB anisotropies have large amplitude than the TSZ contributions. Then, to compare the expected profile with the data, we stack the signal of all the clusters in our sample. The anisotropy is averaged in rings of width  $\theta_{500}/2$ , where  $\theta_{500}$  is the angular scale subtended by the  $r_{500}$ . For each data point an error bar is obtained by evaluating 1,000 times the average profiles at 579 random positions in the SMICA map. To avoid overlapping real and simulated clusters we removed a disc of  $80'$  around each of the clusters in our sample.

Using eqs. (4), (7), (8) and (9), we constructed the pressure profile of all clusters in the data as a function of three parameters:  $(\delta, L, \gamma)$ . We integrated the profiles along the line of sight and convolved them with a Gaussian beam with the same resolution of the SMICA map. We considered two parameterizations. In (A)  $L = \zeta r_{500}$  differs from cluster to cluster but scales linearly with  $r_{500}$ ; in this parametrization we assume that  $\zeta = [0.1, 4]$ . In (B)  $L$  has the same value for all the clusters; it varies in the range  $L = [0.1, 20]$ Mpc, from the scale of a typical core radius to the mean cluster separation. Since if  $\delta < -1$  the potential is repulsive and if  $\delta = -1$  the potential diverges, we took  $\delta = [-0.99, 1.0]$ . Finally, the polytropic index  $\gamma$  was set to vary in the range  $\gamma = [1.0, 1.6]$ , that corresponds to an isothermal and adiabatic monoatomic gas, respectively. We took 30 equally spaced steps in all intervals.

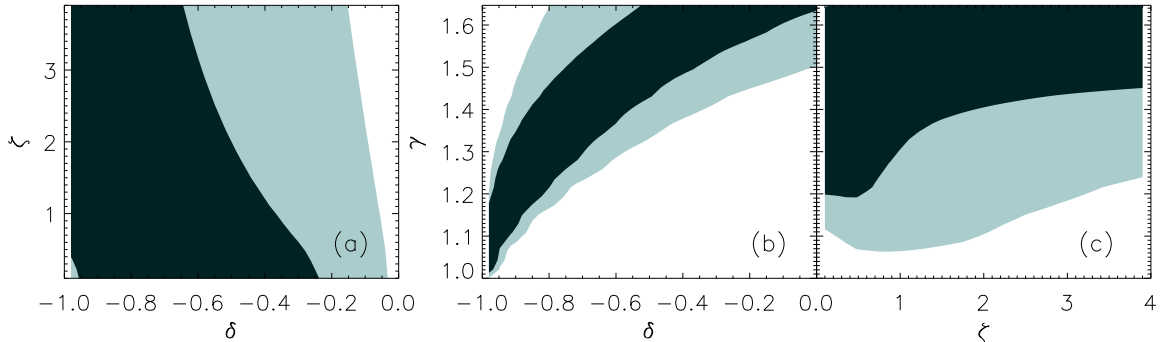


Figure 2: Confidence contours for pairs of parameters of Model A. Contours are at the 68% and 95% confidence level.

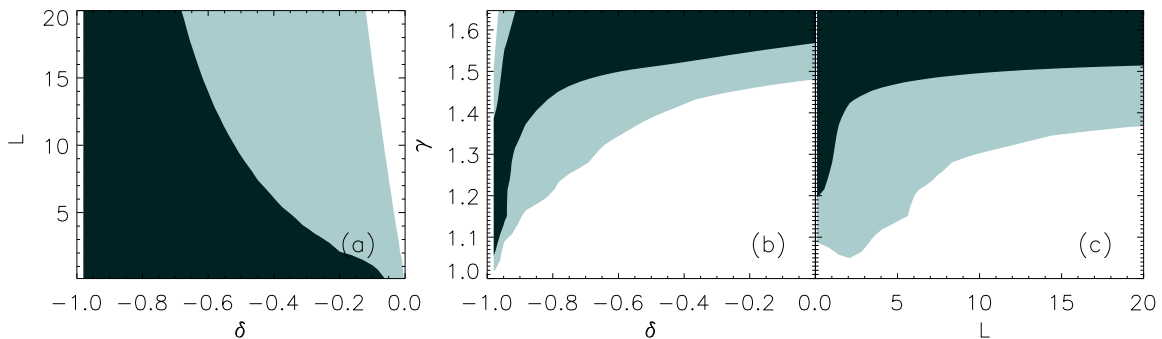


Figure 3: Same as in Fig. 2 for Model B.

## 5. Results and discussion

We computed the likelihood function  $\log \mathcal{L} = -\chi^2/2$  as

$$\chi^2(p) = \sum_{i,j=0}^N (y(p, x_i) - d(x_i)) C_{ij}^{-1} (y(p, x_j) - d(x_j)) \quad (10)$$

where  $N = 7$  is the number of data points, and  $p = (\delta, L, \gamma)$ . In eq. (10),  $d(x_i)$  is the data and  $C_{i,j}$  is the correlation function between the average temperature anisotropy on discs and rings in bins of size  $\theta_{500}$ . The process was computed on 579 random positions outside the cluster locations and repeated 1,000 times.

In Figs. 2 and 3, we computed the 2D contours at the 68% and 95% confidence levels of the marginalized likelihoods of pairs of parameters of Model A and Model B, respectively. Since the contours are not closed, we can only quote the following upper limits at the same level of confidence:  $\delta < -0.46, -0.10$ ,  $\zeta < 2.5, 3.7$  and  $\gamma > 1.35, 1.12$  for Model A and  $\delta < -0.43, -0.08$ ,  $L < 12, 19$  Mpc and  $\gamma > 1.45, 1.2$  for Model B. Notice that  $L$  is similar in both A and B and  $\gamma$  dominated by the physical boundary imposed.

Although model parameters are weakly constrained by the data, the value  $\delta = 0$  is excluded at more than 95% confidence level. Since  $\delta \simeq 0$  corresponds to the standard Newtonian potential without DM, our result indicates that a self-gravitating gas, without DM or modified gravity, does not fit the data.

## 6. Conclusions

We have constrained the analytical  $f(R)$  model of gravity by comparing the pressure profile of clusters of galaxies with CMB data. We have demonstrated that these models can accurately

fit cluster profiles without a potential well dominated by DM. In this context,  $f(R)$  gravity can be considered a viable alternative to DM. Our results also showed that a profile made of gas, without a modified potential or without significant DM contributions could not fit the observed profiles.

Our constraints on model parameters are rather weak since we only used the data on the cluster profile but we did not use the frequency dependence of the TSZ effect, the reason being that the Planck Collaboration has not released foreground cleaned maps at each frequency. Then, our results could be substantially improved when including this frequency information, opening the possibility of constraining - ruling out the modified Newtonian potential at this scale.

## References

- [1] Suzuki N et al 2012 *ApJ* **746**, 85
- [2] Hinshaw G et al 2013 *ApJS* **208**, 19
- [3] Planck Collaboration. “Planck 2013 results. XV. CMB power spectra and likelihood”, 2014 *A&A* **571**, 15
- [4] Planck Collaboration. “Planck 2013 results. XVI. Cosmological parameters”, 2014 *A&A* **571**, 16
- [5] Planck Collaboration. “Planck 2013 results. XX. Cosmology from Sunyaev-Zeldovich cluster counts”, 2014 *A&A* **571**, 20
- [6] Planck Collaboration. “Planck 2013 results. XXI. Cosmology with the all-sky Planck Compton parameter  $y$ -map”, 2014 *A&A* **571**, 21
- [7] Capozziello S and De Laurentis M 2011 *Physics Reports* **509**, 167
- [8] Berry C P L and Gair J L 2011 *Phys Rev D* **83**, 104022
- [9] Capozziello S De Laurentis M de Martino I Formisano M and Odintsov S 2012 *Phys Rev D* **85**, 044022
- [10] Capozziello S and De Laurentis M 2012 *Ann. Phys.* **524**, 1
- [11] Cardone V F and Capozziello S 2011 *MNRAS* **414**, 1301
- [12] Napolitano N R Capozziello S Romanowsky A J Capaccioli M and Tortora C 2012 *ApJ* **748**, 87
- [13] Sunyaev R A and Zeldovich Y B 1972 *Comments on Astrophys. Space Phys.* **4** 173
- [14] Sunyaev R A and Zeldovich Y B 1980 *MNRAS* **190**, 413
- [15] Planck Collaboration. “Planck intermediate results V: Pressure profiles of galaxy clusters from the Planck Survey”, 2013 *A&A* **550**, 131
- [16] Planck Collaboration. “Planck intermediate results X: Physics of the hot gas in the Coma cluster”, 2013 *A&A* **554**, 140
- [17] Planck Collaboration. “Planck 2013 results. XXIX. Planck catalogue of Sunyaev-Zeldovich sources”, 2014 *A&A* **571**, 29
- [18] Navarro J F Frenk C S and White S D M 1997 *ApJ* **490**, 493
- [19] Atrio-Barandela F Kashlinsky A Kocevski D and Ebeling H 2008 *ApJ* **675**, L57
- [20] Arnaud M Pratt G W Piffaretti R Bhringer H Croston J H and Pointecouteau E 2010 *A&A* **517**, 92
- [21] Cavaliere A and Fusco-Femiano R 1976 *A&A* **49**, 137
- [22] Cavaliere A and Fusco-Femiano R 1978 *A&A* **70**, 677
- [23] Jones C and Forman W 1984 *ApJ* **276**, 38
- [24] Sayers J et al 2013 *ApJ* **768**, 177
- [25] Kocevski D and Ebeling H 2006 *ApJ* **645**, 1043
- [26] White D A Jones C and Forman W 1997 *MNRAS* **292**, 419
- [27] Planck Collaboration. “Planck 2013 results. XII. Component separation”, 2014 *A&A* **571**, A12